Beta-IV spectrin autoantibodies as a marker of paraneoplastic neuropathy: A case series [Supplemental Information]

Christopher M. Bartley, M.D., Ph.D.[1,2*], Thomas T. Ngo, B.S.[1,2*], Bonny D. Alvarenga, B.A.[1,3], Andrew F. Kung, B.A.[4], Lindsay H. Teliska, B.S.[5], Michael Sy, M.D.[6], Joseph L. DeRisi, Ph.D.[7,8], Matthew N. Rasband, Ph.D.[5], Sean J. Pittock, M.D.[9,10,11], Divyanhshu Dubey, M.B.B.S.[9,10,11‡], Michael R. Wilson, M.D., M.A.S.[1,3‡], Samuel J. Pleasure, M.D., Ph.D.[1,3‡]

[1] Weill Institute for Neurosciences, University of California, San Francisco, California
[2] Department of Psychiatry and Behavioral Sciences, University of California San Francisco, California
[3] Department of Neurology, University of California, San Francisco, California
[4] University of California San Francisco, School of Medicine, San Francisco, California
[5] Department of Neuroscience, Baylor College of Medicine, Houston, Texas
[6] Department of Neurology, University of California, Irvine, California
[7] Chan Zuckerberg Biohub, San Francisco, California
[8] Department of Biochemistry and Biophysics, University of California, San Francisco, California
[9] Department of Laboratory Medicine and Pathology, Mayo Clinic Foundation, Rochester, Minnesota
[10] Department of Neurology, Mayo Clinic Foundation, Rochester, Minnesota
[11] Center MS and Autoimmune Neurology, Mayo Clinic, Rochester, Minnesota

Supplemental Case Histories

Case 1

A 77-year-old woman with a history of high-grade serous carcinoma of the uterus and fallopian tube developed gait instability and distal lower extremity numbness and paresthesias approximately 6 months after the cancer diagnosis (**eTable 1**). She underwent total abdominal hysterectomy and bilateral oophorectomy and was treated with carboplatin and paclitaxel. On examination she had reduced temperature and pain sensation distally involving her feet and fingers. Vibration and proprioception at the toes were also reduced. Confrontational strength testing revealed bilateral distal foot weakness. Bilateral Achilles deep tendon reflexes were reduced. She had an ataxic wide-based gait and required a walker to ambulate. Nerve conduction studies (NCS) revealed mildly reduced sensory amplitudes along with prolonged distal latencies. She was discharged without immunotherapy but was readmitted to the hospital 3-4 months later due to the development of a subacute encephalopathy. MRI brain was found to be unremarkable. CSF analysis revealed lymphocytic pleocytosis (21 nucleated cells/dL) and elevated CSF protein (73 mg/dL). Electroencephalography revealed generalized delta activity. She was initiated on intravenous solumedrol (1g daily for 5 days) and had significant cognitive improvement. Six months later the patient was re-admitted to the hospital with pneumonia where she died.

Case 2

An 87-year-old woman presented to an outpatient neurology clinic with new onset dizziness and diplopia. Ten years prior to the onset of her neurological symptoms she had been diagnosed with estrogen and progesterone receptor positive, HER2-negative breast adenocarcinoma

(stage I, pT1b, pN0) (**eTable 1**). She was sent to the emergency room out of concern for stroke. MRI of the brain and MRA head and neck with and without contrast was unremarkable, and she was sent home on meclizine. Because her dizziness was persistent, meclizine was increased to 25mg three times a day. Over the next few days, she developed dysarthria, dysphagia requiring tube feeding, bilateral facial numbness, urinary retention, and generalized weakness relegating her to a wheelchair. She presented to the emergency room again. Serum RPR, vitamin B12, methylmalonic acid, CK, and CRP were within normal limits. Serum autoimmune testing for ANCA, ANA, RF, anti-AChR antibodies, anti-MUSK antibodies, and cryoglobulins was negative. CSF studies were not obtained at this time. After another unremarkable MRI of her brain with contrast, she was suspected to have Miller-Fisher variant of Guillian-Barré Syndrome and she was treated empirically with intravenous immunoglobulin (IVIg) (0.4g/kg daily for 5 days). By day 3 of IVIg treatment, her diplopia, dysphagia, and dysarthria began to improve. She was discharged to a rehabilitation facility and eventually home where she was able to take a few steps and no longer required tube feeding. Over the next 4 months, her symptoms returned with bilateral ptosis, dysphagia, dysarthria, facial numbness, urinary retention, and lower extremity weakness again requiring a wheelchair. She again presented to the emergency room, and she received another round of IVIg (0.4g/kg daily x 5 days) which did not improve her symptoms. She was discharged to a rehabilitation center.

Two weeks later, she was readmitted to the hospital due to worsening dysarthria and leg weakness. Examination at that time, demonstrated bilateral ptosis, ophthalmoplegia (limited bilateral abduction and adduction), and sensory loss over maxillary (V2) and mandibular (V3) trigeminal dermatomes and dysarthria. Strength assessment revealed proximal weakness involving the bilateral lower extremities (bilateral hip-flexion 1/5 [medical research council, MRC[1]], bilateral knee extension and flexion 2/5 [MRC]). Distal lower extremity strength was normal. Sensory exam revealed decreased vibration sensation involving the upper and lower extremities, but other sensory modalities were intact. Deep tendon reflexes were absent in the lower extremities but preserved in the upper extremities.

During her second hospital admission, repeat MRIs of the brain, cervical and thoracic spine with and without contrast were unremarkable. CSF analysis showed mildly elevated protein at 59 mg/dL (reference: 15 - 45 mg/dL) and 3 nucleated cells (reference: 0-5 per mm^3). CSF glucose was 66 mg/dL (serum glucose 120 mg/dL), LDH <25 U/L, CSF cultures and gram stain were negative, and CSF paraneoplastic panel testing (PAC1) did not detect any informative autoantibodies. Immunofixation of protein in both serum and CSF along with repeat anti-AChR and anti-MuSK antibody testing was negative. MRI of bilateral femurs demonstrated asymmetric intramuscular edema within the adductor/obturator externus muscles (more pronounced on the right side). A NCS revealed absent sural responses (blink reflexes not tested). Needle electromyography demonstrated increased insertional activity (fibrillations) and myopathic motor units in the proximal upper (deltoid and biceps) and lower extremity (vastus lateralis) muscle. Biopsy of the left vastus lateralis revealed scattered angular and atrophic fibers without significant inflammatory infiltrates. An inflammatory myositis panel was negative. There was no evidence of breast cancer recurrence by mammogram or CT chest, abdomen, and pelvis.

She was again trialed on IVIg (0.4 g/kg daily x 5 days). After the initial IVIg infusions, she regained the ability to ambulate with assistance, and her dysphagia had improved. She was discharged from the hospital but neurologically declined shortly thereafter. Subsequent rounds

of IVIg were ineffective, and other immunotherapies were not tried. On follow-up examination approximately 5 months after symptom onset, she had significantly worse bilateral upper extremity weakness (MRC grade 3/5), persistent lower extremity weakness, and was diffusely areflexic. Her symptoms progressed, and she died a few days later.

Supplemental Discussion

Discussion

Nearly half of cancer patients develop peripheral neuropathy that is typically attributed to a combination of chemotherapeutic toxicity, metabolic derangements, tumor infiltration of nerves, or cachexia[2]. In addition, paraneoplastic syndromes can cause neuropathy, though this is thought to occur in less than 1% of patients with cancer.[3] The diagnosis of paraneoplastic neuropathy can lead to earlier cancer detection, guide chemotherapeutic treatment decisions, prompt initiation of immunomodulatory therapy, and may be useful for longitudinal autoantibody monitoring as part of cancer surveillance. While anti-Hu and anti-CV2/CRMP5 antibodies are the most common diagnostic biomarkers for paraneoplastic neuropathy[4], nearly three quarters of carcinoma-associated paraneoplastic neuropathies may be seronegative[2, 5] — highlighting an unmet need for additional diagnostic biomarkers.

In this study, we used an anatomic assay to prioritize PhIP-Seq-enriched antigens and subsequently validated anti-βIV spectrin antibodies in two individuals with suspected paraneoplastic neuropathy. Although there is a prior report of βIV spectrin paraneoplastic motor neuropathy[6, 7], the absence of subsequent cases has obscured the diagnostic utility of βIV spectrin autoantibodies. Here, we identified two additional cases with overlapping clinical presentations. We searched a large database of thousands of PhIP-Seq screens and did not identify further examples of βIV spectrin autoantibodies in the healthy population or in patients with other neuroinflammatory conditions. We failed to validate anti-ankyrin G antibodies in case 1 using two direct binding assays despite enrichment by PhIP-Seq. This suggests that ankyrin G may have been indirectly enriched by nonspecific bead binding or peptide-peptide interactions[8]. Taken together, these data indicate that, while rare, anti-βIV spectrin antibodies are specific biomarkers of paraneoplastic neuropathy[9].

Notably, we detected βIV spectrin antibodies in the CSF of both patients. Case 1 later developed CSF pleocytosis and steroid responsive subacute encephalopathy with generalized slowing on EEG. Case 2 had evidence for a sensorimotor neuropathy and myopathy with bulbar muscle and nerve involvement. The previously reported single case was not tested for CSF βIV antibodies, however CSF-restricted oligoclonal bands and cervical T2 hyperintensities were reported. Therefore, in some cases βIV spectrin antibodies may also be associated with central nervous system (CNS) pathology and clinical syndromes.

Indeed, CNS pathology is observed in many individuals with congenital βIV spectrinopathy including choreoathetoid movements, intellectual disability, seizures, and nonconvulsive EEG abnormalities[10, 11]. However, the core feature of congenital βIV spectrinopathy appears to be motor axonal neuropathy with attendant muscle atrophy and areflexia.[10-12] All three reported βIV spectrin paraneoplastic neuropathy cases presented with weakness and hyporeflexia, with fibrillations documented in the two patients who were evaluated by EMG. Our case 2 also had biopsy-proven muscle fiber atrophy without evidence of myositis or vasculitis. Surprisingly, NCS results in patients with symptomatic βIV spectrinopathy are variable, with some having completely normal findings.[11] Although NCS studies in paraneoplastic neuropathies are typically remarkable, NCS in our patients did not reflect the degree of clinical impairment—similar to βIV spectrinopathothies.

Autoantibodies targeting the NoR are most commonly associated with chronic inflammatory demyelinating polyneuropathy (CIDP).[13] Of those autoantigens, only neurofascin 186 (NF186) is

139 expressed at both the AIS and NoR.[14, 15] Importantly, our two patients as well as the previously
140 reported patient had peripheral neuropathy without clear-cut electrodiagnostic evidence of
141 demyelination and therefore do not meet the clinical diagnosis of CIDP. Future studies should
142 investigate whether there are special features of the AIS and NoR that make them particularly
143 immunogenic.

144 The pathophysiology of anti-βIV autoantibodies is unclear. CIDP-associated autoantibodies
145 primarily target proteins with extracellular epitopes including neurofascins, contactin 1, and
146 CASPR[13]. Like many paraneoplastic autoantigens, βIV spectrin is an intracellular protein —
147 which is typically thought to reflect a T cell-mediated pathophysiology. However, βIV spectrin Σ1
148 and Σ6 each harbor a phosphoinositide-binding pleckstrin homology domain that mediates their
149 association with the cytoplasmic plasma membrane. Because autoantibodies that target the
150 cytoplasmic membrane protein amphiphysin have been reported to be pathogenic[16], we cannot
151 exclude the possibility that βIV spectrin antibodies are also pathogenic. Unfortunately, there was
152 insufficient CSF and sera to test patient βIV spectrin antibodies against live neurons.

153 Overall, these data further support the consideration of βIV spectrin antibodies in the diagnostic
154 evaluation of cancer-associated peripheral neuropathy.

155 **Limitations:**

156 This study is limited by the small number of cases. Although both patients presented here have
157 overlapping clinical features, they are not identical. Additional clinical data for case 1 were
158 unavailable (including timing of chemotherapeutic treatment initiation relative to the onset of
159 neuropathy), thereby limiting the completeness of the clinical description. Nonetheless, our
160 evaluation of hundreds of biospecimens by tissue-based assay and thousands of biospecimen
161 by PhIP-Seq indicate that anti-βIV spectrin antibodies are rare, and preferentially occur patients
162 with peripheral neuropathy with or without additional neurologic symptoms. Separately,
163 antibodies targeting neurofascin, which is expressed at both the AIS and NoR, are associated
164 with CIDP. Although we did not directly test for anti- neurofascin antibodies by cell-based assay,
165 in neither case was the NCS consistent with CIDP, and neurofascin was not enriched by PhIP-
166 Seq. Finally, although these antibodies are unlikely to be directly pathogenic owing the βIV
167 spectrin's intracellular localization, we were unable to test this directly due to insufficient CSF
168 and serum.

169 **Supplemental Tables**

170 **eTable 1.**

Antigen	**Beta IV Spectrin**	
Case	**Case 1**	**Case 2**
Age/Sex	77F	87F
Cancer	High-grade serous carcinoma of the fallopian tube and uterus	ER^+/PR^+, $HER2^-$ breast adenocarcinoma (stage 1, pT1b, pN0)
Clinical Features	Ataxic wide based gait requiring a walker to ambulate. Distal foot weakness. Distal lower extremity numbness and paresthesias. Reduced temperature and pain sensation distally involving her feet and fingers. Reduced vibration and proprioception at the toes. Reduced Achilles deep tendon reflexes bilaterally. Subacute encephalopathy	Dizziness, diplopia, dysarthria, dysphagia. Generalized weakness (bilateral upper extremity weakness, bilateral lower extremities, bilateral hip-flexion, bilateral knee extension and flexion). Distal lower extremity strength was normal. Bilateral facial numbness. Decreased vibration sensation involving upper and lower extremities, other sensory modalities were intact. Deep tendon reflexes absent in the lower extremities, preserved in the upper extremities. Urinary retention.
EEG	Generalized delta activity	N.D.
Imaging		
MRI w/wo contrast: Brain	Normal	Normal x 2
MRI w/wo contrast: Cervical and thoracic spine	N.D.	Normal
MRI: Bilateral femurs	N.D.	asymmetric intramuscular edema within the adductor/obturator externus muscles
CT: Chest, Abdomen, Pelvis	N.D.	No evidence of cancer recurrence
Electrodiagnostics		
NCS	Mildly reduced sensory amplitudes along with prolonged distal latencies	Absent sural response

EMG	N.D.	Increased insertional activity (fibrillations) and myopathic motor units in the proximal upper (deltoid and biceps) and lower extremity (vastus lateralis) muscle
Muscle Biopsy	N.D.	Left vastus lateralis: scattered angular and atrophic fibers without significant inflammatory infiltrates
CSF		
WBC Cell Count (cells/mm^3)	21	3
Protein (mg/dL)	73	59
Glucose (CSF/serum ratio)	Unknown	0.55
CSF IgG	Unknown	N.D
IgG index	Unknown	N.D.
OCBs	Unknown	N.D.
LDH	Unknown	<25 U/L
Gram Stain	Unknown	Negative
Bacterial Cultures	Unknown	No growth at 7 days
Fungal Cultures	Unknown	No growth at 28 days
Mycobacterium Tuberculosis Cultures (AFB)	Unknown	No growth at 59 days
Negative Autoantibody Testing	CSF Autoimmune encephalopathy panel (ENC2): LGI1, CASPR2, NMDA-R, GABA-B, DPPX, Amphiphysin, AGNA1, ANNA1 (anti-Hu), ANNA2 (Nova 1/anti-Ri), ANNA3, CRMP-5, anti-Tr, PCA1 (anti-Yo), PCA2 Serum paraneoplastic panel: Amphiphysin, AGNA1, ANNA1 (anti-Hu), ANNA2 (Nova 1/anti-Ri), ANNA3, CRMP-5, anti-Tr, PCA1 (anti-Yo), PCA2	CSF Paraneoplastic Panel (PAC1): Amphiphysin, AGNA1, ANNA1 (anti-Hu), ANNA2 (Nova 1/anti-Ri), ANNA3, CRMP-5, anti-Tr, PCA1 (anti-Yo), PCA2 Serum ANCA, ANA, RF, and cryoglobulins Serum Anti-AChR and anti-MuSK (tested twice) Serum inflammatory Myositis Panel: anti-PM/Scl-100, Jo-1, ss-A, U1-RNP, EJ, Ku, MDA-5, MI-2, OJ, SRP, TIF 1 Gamma, and U2 snRNP antibodies
Treatment/Response	1g daily for 5 days, significant cognitive improvement	1st: 0.4g/kg daily for 5 days, improved 2nd: 0.4g/kg daily for 5 days, no improvement

		3rd: 0.4/kg daily for 5 days, no improvement

N.D. = Not done.

192 **Supplemental Figures**

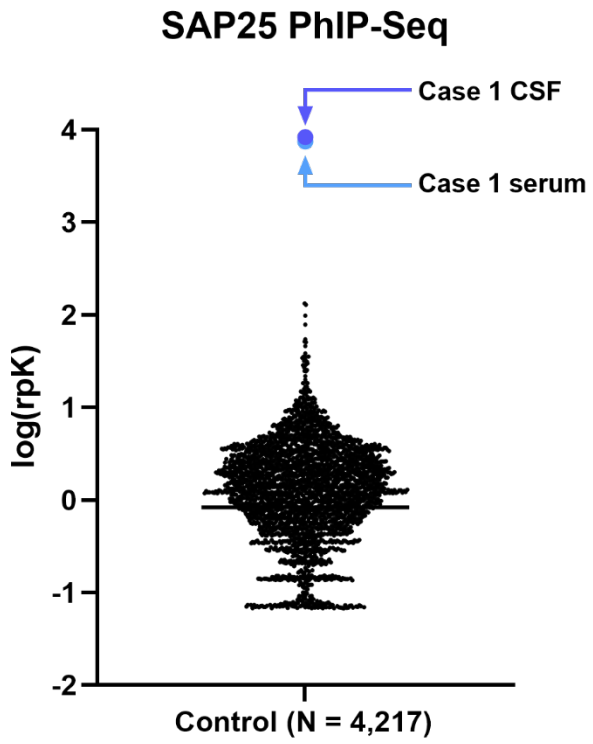

193

194 **eFigure1. Case 1 CSF and sera enrich SAP25.** Logarithmic dot plot of total SAP25 enrichment
195 by PhIP-Seq. For case 1, each point represents the mean of technical replicates. The z-score of
196 log(rpK) = 7.3 for case 1 CSF and 7.2 for case 1 serum.

197

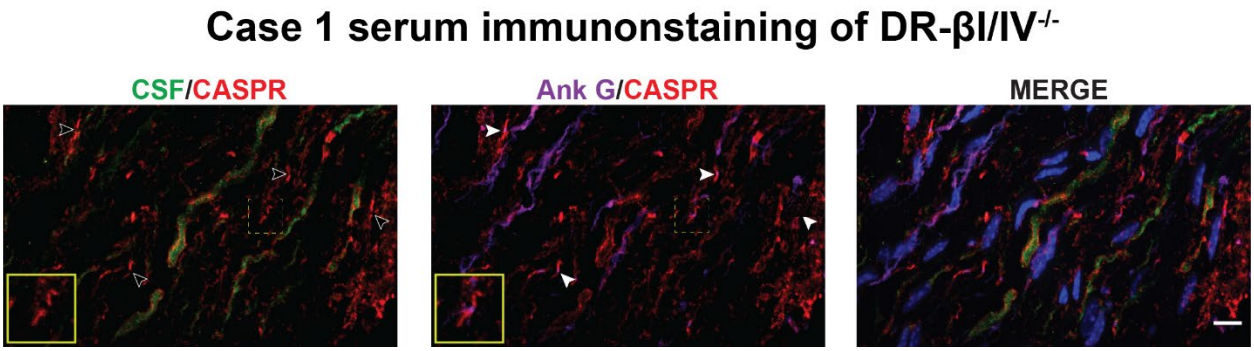

eFigure 2. Case 1 serum IgG does not immunostain ankyrin G-expressing βI/βIV deficient NoR. DR-βI/βIV$^{-/-}$ tissue was immunostained with serum from case 1 at a 1:1000 dilution. Case 1 serum IgG fails to immunostain βI/βIV-deficient NoR (left) that express ankyrin G (middle). The yellow insets correspond to the dotted square in the same panel. Empty arrowheads indicate the absence of nodal serum IgG staining while filled arrowheads indicate nodal ankyrin G staining. Scale bar = 10μm.

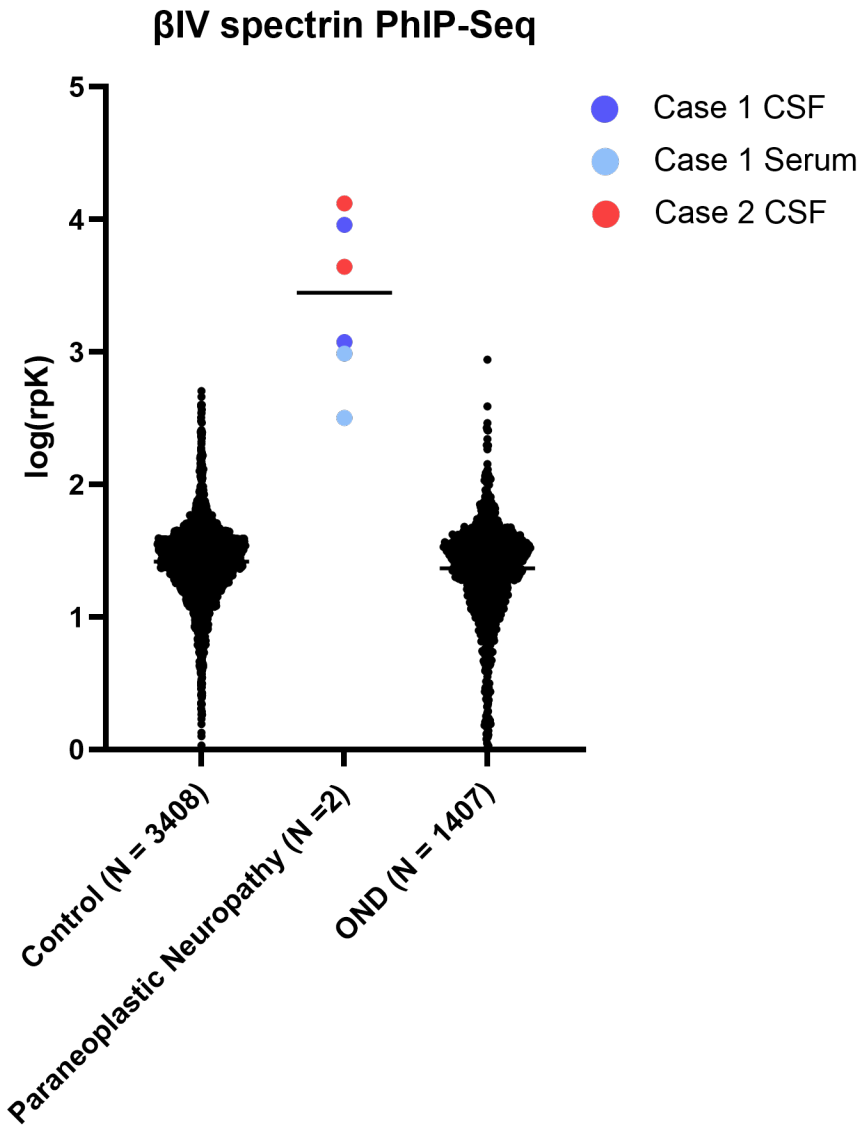

eFigure 3. Case 1 and 2 CSF enrich βIV spectrin by PhIP-Seq more so than all other controls and neurologic and neuroinflammatory subjects. For each PhIP-Seq screen, the total rpK for βIV spectrin was calculated and plotted on a logarithmic dot plot. For case 1 and 2, technical replicates are shown as individual points. For each group, the horizonal line represents the median of the total rpK. Control samples are comprised of beads only and CSF, serum, and plasma samples from health controls including technical replicates. OND represents CSF, serum, and plasma from patients with other neurologic and neuroinflammatory disorders including technical replicates. For technical replicates of patients samples, Z-scores of mean log(rpK) relative to control and OND respectively were calculated as 4.5 and 2.8 for case 1 serum, 7.5 and 4.4 for case 1 CSF, and 8.2 and 4.8 for case 2 CSF.

Supplemental Materials and Methods

Patients

This study was approved by Mayo Clinic Institutional Review Board (IRB) numbers 08-006647 and 08-007846. As patients were deceased, informed consent waivers could not be obtained. The IRB's were approved under informed consent waiver criteria [45 CFR 46.116(d)]:

(1) The research involves no more than minimal risk to the subjects;
(2) The waiver or alteration will not adversely affect the rights and welfare of the subjects;
(3) The research could not practicably be carried out without the waiver or alteration; and
(4) Whenever appropriate, the subjects will be provided with additional pertinent information after participation.

The relevant IRBs were further approved in consideration of HIPAA waiver criteria [45 CFR Part 164 - Security and Privacy Rule, Subpart E]:

(1) The use or disclosure of PHI involves no more than minimal risk to the privacy of individuals, based on the presence of at least the following elements:

- *An adequate plan to protect the identifiers from improper use and disclosure;*
- *An adequate plan to destroy the identifiers at the earliest opportunity consistent with the conduct of the research, unless there is a health or research justification for retaining the identifiers or such retention is otherwise required by law; and*
- *Adequate written assurances that the PHI will not be reused or disclosed to any other person or entity, except as required by law, for authorized oversight of the research study, or for other research for which the use or disclosure of PHI would be permitted by HIPAA.*

(2) The research could not practicably be conducted without the waiver or alteration.
(3) The research could not practicably be conducted without access to and use of the PHI.

For this study, 264 archived specimens (158 sera, 106 CSF) tested by mouse tissue indirect immunofluorescence assay (IFA) at the Mayo Neuroimmunology Laboratory between 2007 and 2020 with a filamentous IgG staining pattern were retested to identify axonal initial segment (AIS) immunoreactivity. AIS staining was seen in 37 samples corresponding to 28 patients (9 serum only, 11 CSF only, 8 both). Autoantigenic target for 33 samples with identical starting was confirmed to be TRIM46[17]. Two of the remaining three samples with identical staining pattern of the AIS in cerebellum, cerebral cortex and hippocampus on murine brain were shared with UCSF for putative autoantigen detection. CSF TIFA endpoint for cases 1 and 2 were 1:256 and 1:4, respectively.

Mayo Clinic tissue immunofluorescence assay for AIS immunoreactivity

Patient CSF were tested on a cryosectioned (4 μm) composite of adult mouse tissues: cerebellum, midbrain, cerebral cortex, hippocampus, kidney and gut. Sections were fixed using 4% paraformaldehyde for 1 minute, then permeabilized with 3-[(3-cholamidopropyl) dimethylammonio]-1-propanesulfonate (CHAPS), 0.5%, in phosphate buffered saline (PBS, for 1 minute), and then blocked for 1 hour with normal goat serum (10% in PBS). After PBS-rinse,

258 patient specimen was applied (serum was pre-absorbed with bovine liver powder, 1:240 dilution,
259 and CSF was non-absorbed, 1:2 dilution). After 40 minutes, and PBS wash, a species-specific
260 secondary antibody conjugated with fluorescein isothiocyanate (FITC, 1:100) was applied
261 (Southern Biotechnology Associates, Inc, Birmingham, AL, USA). Cover slips were mounted
262 using ProLong Gold antifade medium (containing DAPI; Molecular Probes Thermo Fisher
263 Scientific, USA). Fluorescence images were captured using Olympus BX51 polarizing
264 microscope with Olympus DP73 high-performance Peltier-cooled, 17.28 megapixel camera.
265 Patient specimens yielding positive results were titrated in doubling dilutions to determine the
266 endpoint of autoantibody detection.
267

268 Animals

269 Post-natal day 40 – 60 mice from the F1 cross of FVB (Jackson Laboratory, Cat. No. #001800)
270 x C57BL/6J (The Jackson Laboratory, Cat. No. #000664) mice were used for initial tissue-based
271 assays. All procedures used in this study complied with federal guidelines and the institutional
272 policies of the University of California San Francisco Institutional Animal Care and Use
273 Committee.

274 Advillin$^{Cre/+}$ and Chat$^{Cre/+}$ *Ank3* tissue and Advillin$^{Cre/+}$ *Sptn/Sptbn4* tissues were a generous gift
275 from Matthew Rasband of Baylor College of Medicine.

276

277 UCSF Tissue-based assays

278 Mice were transcardially perfused with 4% paraformaldehyde (PFA) and brains post-fixed in 4%
279 PFA overnight. After 30% sucrose equilibration, brains were blocked in OCT and sectioned at
280 12 µm. Following rehydration in TBS-T (0.1% Tween-20), the sections were incubated in 70%
281 ethanol containing TrueBlack® Lipofuscin Autofluorescence Quencher (Biotium, #23007) at
282 1:20, then washed several times using TBS-T.

283 Sections were permeabilized and blocked in TBS-T containing 10% lamb serum and 0.1%
284 Triton X-100. Sections were then incubated with patient CSF or sera at 4°C overnight. Sections
285 were rinsed at least 5x with TBS-T and counterstained with anti-human IgG (Alexa Fluor 488)
286 for one hour. Nuclei were stained with DAPI at 1:2000 and stained sections were coverslipped
287 with ProLong Gold Antifade (ThermoFisher, Cat No. P36930) or Prolong Diamond Antifade
288 (ThermoFisher, Cat No. P36961).

289

290 Immunostaining of conditional knockout tissue

291 *Ank3* and *Sptbn/Sptbn4* conditional knockout tissues were stained using the same procedure
292 described above for tissue-based assays. Tissues were stained using sera at 1:1000 and CSF
293 at 1:4, anti-Caspr 1:1000, anti-Ankyrin-G 1:500, and anti-SPBTN4 1:500.

294

295 Phage Display Immunoprecipitation Sequencing (PhIP-Seq)

296 PhIP-Seq screens and peptide alignments were performed as previously described[18]. For
297 analysis, peptide counts were converted to reads per one hundred thousand (rpK) to account for

298 differences in sequencing depth. For each protein, peptide rpKs were summed and divided by
299 the total number peptides mapping to that protein (length normalization), thereby accounting for
300 larger proteins having a higher total rpK due to nonspecific phage:bead binding. For a given
301 protein, enrichments were represented as the mean of the length-normalized total rpK of
302 technical replicates.

303 For Figure 3A, European Molecular Biology Laboratory Bioinformatics Institute (EMBL-EBI)
304 definitions were used to define AIS (GO:0033268) and NoR (GO:0043194) proteins[19, 20].
305 Because AIS and NoR staining was observed in both cases, only those proteins defined as both
306 AIS and NoR proteins were included in the analysis (i.e. proteins defined as only either an AIS
307 or a NoR protein were excluded).

308

309 HEK293 Overexpression Assay

310 HEK293 cells were plated onto 10mm poly-d-lysine coated (50µg/mL) glass coverslips in
311 24-well plates. HEK293 cells were transfected overnight with ankG-mCherry (Addgene,
312 #42566), pCS-MT-Myc-SPTBN4-Σ1 or pCS-MT-Myc-SPTBN4-Σ6 plasmids using
313 Lipofectamine 3000 (ThermoFisher). The following day, after two rinses with ice cold 1X PBS,
314 transfected cells were fixed were 4% PFA for 10 minutes. The fixed cells were rinsed with PBS,
315 blocked with 5% lamb serum in PBS, and permeabilized for 30 minutes using with blocking
316 buffer containing 0.5% Triton. Fixed cells were incubated overnight at 4°C with CSF at 1:4 in 5%
317 blocking buffer, and a commercial anti-Myc-tag antibody, if necessary. The cells were rinsed
318 with PBS four times, and stained with Alexa Fluor secondaries at a 1:1000 dilution in 5%
319 blocking buffer. Nuclei were stained with DAPI at 1:2000 in PBS for 5 minutes. Stained slides
320 were then mounted onto microscope slides with Prolong Diamond Antifade (ThermoFisher, Cat
321 No. P36961)

322

323 Expression plasmids

Vector	Additional Details
ankG-mCherry	Addgene, Plasmid #42566
pCS-MT-Myc-SPTBN4-Σ1	Gift from Matthew Rasband, Baylor College of Medicine
pCS-MT-Myc-SPTBN4-Σ6	Gift from Matthew Rasband, Baylor College of Medicine

324
325 Antibodies

Primary Antibodies			
Name	**Host Species**	**Vendor (Catalog No.)**	**Assay (Concentration)**

Anti-Myc-Tag mAb, 71D10	rabbit	Cell Signaling Technology *(#2278)*	ICC-IF (1:200)
Anti-Caspr pAb	rabbit	Abcam (ab34151)	ICC-IF (1:1000) IHC-F (1:1000)
Anti-SPTBN4 mAb, clone N393/76	mouse	NeuroMab (75-377)	ICC-IF (1:500) IHC-F (1:500)
Anti-Ankyrin-G mAb, clone 106/36	mouse	NeuroMab (75-146)	ICC-IF (1:500) IHC-F (1:500)
Secondary Antibodies			
Fluorophore	**Specifications**	**Vendor (Catalog No.)**	**Assay (Concentration)**
Alexa Fluor 488	AffiniPure Donkey Anti-Human IgG (H+L)	Jackson ImmunoResearch (709-545-149)	ICC-IF (1:1000) IHC-F (1:1000)
Alexa Fluor 594	AffiniPure Donkey Anti-Rabbit IgG (H+L)	Jackson ImmunoResearch (711-585-152)	ICC-IF (1:1000) IHC-F (1:1000)
Cy™ 5	AffiniPure Donkey Anti-Mouse IgG (H+L)	Jackson ImmunoResearch (715-175-151)	ICC-IF (1:1000) IHC-F (1:1000)

326

327 Imaging and Microscopy
328 Panoramic images of tissue stains were acquired at 20X using a Zeiss Axio Scan Z.1 Slide
329 Scanner. Tissue and cell-based assays were imaged at 60X or 100X at the UCSF Nikon
330 Imaging Center with a Nikon CSU-W1 spinning disk confocal microscope, equipped with an
331 Andor Zyla sCMOS camera. Images were prepared using ImageJ (Version 2.1.0/1.53c).

332

333 Data Availability

334 Data, including raw PhIP-Seq sequencing data, are available upon request.

335 Data Analyses, Software, and Figure

336 After peptide alignment, PhIP-Seq data analyses were performed in R and visualized using
337 Graphpad Prism. Figures were drafted in Adobe Photoshop and Illustrator.

338 **References**

339 1. Kleyweg RP, van der Meché FG, Schmitz PI. Interobserver agreement in the assessment of
340 muscle strength and functional abilities in Guillain-Barré syndrome. Muscle Nerve 1991;14:1103-1109.
341 2. Antoine JC, Mosnier JF, Absi L, Convers P, Honnorat J, Michel D. Carcinoma associated
342 paraneoplastic peripheral neuropathies in patients with and without anti-onconeural antibodies. J
343 Neurol Neurosurg Psychiatry 1999;67:7-14.
344 3. Graus F, Reñé R. Paraneoplastic neuropathies. Eur Neurol 1993;33:279-286.
345 4. Dubey D, Lennon VA, Gadoth A, et al. Autoimmune CRMP5 neuropathy phenotype and outcome
346 defined from 105 cases. Neurology 2018;90:e103-e110.
347 5. Forsyth PA, Dalmau J, Graus F, Cwik V, Rosenblum MK, Posner JB. Motor neuron syndromes in
348 cancer patients. Ann Neurol 1997;41:722-730.
349 6. Berghs S, Ferracci F, Maksimova E, et al. Autoimmunity to beta IV spectrin in paraneoplastic
350 lower motor neuron syndrome. Proc Natl Acad Sci U S A 2001;98:6945-6950.
351 7. Ferracci F, Fassetta G, Butler MH, Floyd S, Solimena M, De Camilli P. A novel antineuronal
352 antibody in a motor neuron syndrome associated with breast cancer. Neurology 1999;53:852-855.
353 8. Wu C-H, Liu IJ, Lu R-M, Wu H-C. Advancement and applications of peptide phage display
354 technology in biomedical science. Journal of Biomedical Science 2016;23:8.
355 9. Graus F, Vogrig A, Muniz-Castrillo S, et al. Updated Diagnostic Criteria for Paraneoplastic
356 Neurologic Syndromes. Neurol Neuroimmunol Neuroinflamm 2021;8.
357 10. Wang C-C, Ortiz-González XR, Yum SW, et al. βIV Spectrinopathies Cause Profound Intellectual
358 Disability, Congenital Hypotonia, and Motor Axonal Neuropathy. The American Journal of Human
359 Genetics 2018;102:1158-1168.
360 11. Buelow M, Süßmuth D, Smith LD, et al. Novel bi-allelic variants expand the SPTBN4-related
361 genetic and phenotypic spectrum. European Journal of Human Genetics 2021;29:1121-1128.
362 12. Häusler MG, Begemann M, Lidov HG, Kurth I, Darras BT, Elbracht M. A novel homozygous splice-
363 site mutation in the SPTBN4 gene causes axonal neuropathy without intellectual disability. Eur J Med
364 Genet 2020;63:103826.
365 13. Cortese A, Lombardi R, Briani C, et al. Antibodies to neurofascin, contactin-1, and contactin-
366 associated protein 1 in CIDP: Clinical relevance of IgG isotype. Neurol Neuroimmunol Neuroinflamm
367 2020;7.
368 14. Hedstrom KL, Xu X, Ogawa Y, et al. Neurofascin assembles a specialized extracellular matrix at
369 the axon initial segment. J Cell Biol 2007;178:875-886.
370 15. Davis JQ, Lambert S, Bennett V. Molecular composition of the node of Ranvier: identification of
371 ankyrin-binding cell adhesion molecules neurofascin (mucin+/third FNIII domain-) and NrCAM at nodal
372 axon segments. J Cell Biol 1996;135:1355-1367.
373 16. Werner C, Pauli M, Doose S, et al. Human autoantibodies to amphiphysin induce defective
374 presynaptic vesicle dynamics and composition. Brain 2016;139:365-379.
375 17. Valencia-Sanchez C, Knight AM, Hammami MB, et al. Characterisation of TRIM46 autoantibody-
376 associated paraneoplastic neurological syndrome. J Neurol Neurosurg Psychiatry 2021.
377 18. Song E, Bartley CM, Chow RD, et al. Divergent and self-reactive immune responses in the CNS of
378 COVID-19 patients with neurological symptoms. Cell Rep Med 2021;2:100288.
379 19. Binns D, Dimmer E, Huntley R, Barrell D, O'Donovan C, Apweiler R. QuickGO: a web-based tool
380 for Gene Ontology searching. Bioinformatics 2009;25:3045-3046.
381 20. Huntley RP, Sawford T, Mutowo-Meullenet P, et al. The GOA database: gene Ontology
382 annotation updates for 2015. Nucleic Acids Res 2015;43:D1057-1063.